Biocompatible ferroelectric (Na,K)NbO3 nanofibers — **Source link**

Abolfazl Jalalian, Alexander M. Grishin

Related papers:

- Piezoelectricity and electrostriction in biocompatible (Na,K)NbO3 nanofiber scaffolds

- High Quality Mn-Doped (Na,K)NbO3 Nanofibers for Flexible Piezoelectric Nanogenerators

- Study on synthesis and evolution of sodium potassium niobate ceramic powders by an oxalic acid-based sol–gel method

- 1.6 V Nanogenerator for Mechanical Energy Harvesting Using PZT Nanofibers

- Potassium-sodium niobate lead-free piezoelectric materials: past, present, and future of phase boundaries.

Share this paper:

View more about this paper here: https://typeset.io/papers/biocompatible-ferroelectric-na-k-nbo3-nanofibers-ult5snhdfw

1-1-2012

Biocompatible ferroelectric (Na,K)NbO3 nanofibers

A Jalalian
University of Wollongong, aj393@uowmail.edu.au

A M. Grishin
KTH Royal Institute of Technology, Kista, Sweden

Recommended Citation

Biocompatible ferroelectric (Na,K)NbO3 nanofibers

Abstract

"Dense homogeneous textile composed from continuous bead-free sodium potassium niobate (NKN) nanofibers 100 mu m long and 50-200 nm in diameter was sintered by sol-gel calcination assisted electrospinning. High resolution electron microscopy and x-ray diffraction revealed preferential cube-on-cube growth of fibers in [001] direction. Raman spectrum of NKN fibers contains all the features characteristic to electrically poled orthorhombic phase. In contrast to polycrystalline ceramics, it shows relative enhancement of the Raman cross section of isotropic $A_{1g}(\nu_1)$ mode compared with polar axis defined $F_{2g}(\nu_5)$ and $E_g(\nu_2)$ vibrations. We interpret this as an evidence for superparaelectric state of NKN nanofibers. Spontaneous polarization inside highly crystalline nanofiber exists at room temperature though big distance between fibers prevents the settling of a net macroscopic polarization. (C) 2012 American Institute of Physics. [doi: 10.1063/1.3673282]"

Keywords

nbo3, k, nanofibers, na, biocompatible, ferroelectric

Disciplines

Engineering | Science and Technology Studies

Publication Details

Biocompatible ferroelectric (Na,K)NbO$_3$ nanofibers

A. Jalalian[1,2] and A. M. Grishin[1,a)]

[1]*Department of Condensed Matter Physics, KTH Royal Institute of Technology, SE-164 40, Kista, Sweden*
[2]*University of Wollongong, North Wollongong, NSW 2500, Australia*

Dense homogeneous textile composed from continuous bead-free sodium potassium niobate (NKN) nanofibers 100 μm long and 50-200 nm in diameter was sintered by sol-gel calcination assisted electrospinning. High resolution electron microscopy and x-ray diffraction revealed preferential cube-on-cube growth of fibers in [001] direction. Raman spectrum of NKN fibers contains all the features characteristic to electrically poled orthorhombic phase. In contrast to polycrystalline ceramics, it shows relative enhancement of the Raman cross section of isotropic $A_{1g}(v_1)$ mode compared with polar axis defined $F_{2g}(v_5)$ and $E_g(v_2)$ vibrations. We interpret this as an evidence for superparaelectric state of NKN nanofibers. Spontaneous polarization inside highly crystalline nanofiber exists at room temperature though big distance between fibers prevents the settling of a net macroscopic polarization. © 2012 American Institute of Physics. [doi:10.1063/1.3673282]

In 1949, Matthias had grown in Bell Labs sodium and potassium niobate (called that time as a columbate) perovskite single crystals, discovered piezoelectricity, birefringence, dielectric hysteresis loop, and polymorphic phase transition below their Curie points.[1] In 1955, Shirane had built phase diagram of continuous solid solution of NaNbO$_3$ and KNbO$_3$ (Na$_x$K$_{1-x}$NbO$_3$, hereinafter NKN) that explained a contradiction between observed dielectric and structural properties. Although "induced ferroelectricity" occurs in NaNbO$_3$ in a strong electric field only, a small addition of KNbO$_3$ to pure NaNbO$_3$ gives a birth to ferroelectric phase when $x < 0.97$.[2] Egerton[3] and Dungan[4] showed NKN combines dielectric permittivity around 400, resistivity 10^{12} $\Omega \times$ cm, and piezoelectric constant d_{33} as high as 160 pC/N. These properties achieved at morphotropic phase boundary $x = 0.5$ promise NKN for solid ultrasonic delay line use.

Ferroelectric NKN was patented as a biocompatible material for implants. Thorough toxicology test showed there were no any bacterial products (endotoxin) appear as well as viability of human monocytes was not negatively affected by the presence of NKN ceramics.[5]

Although NKN films were cathode sputtered more than two decades ago,[6] volatility of alkaline elements impeded high-yield fabrication of NKN films for a long time. In late 1990s high performance NKN films had been grown by rf-magnetron sputtering[7] and pulsed laser deposition (PLD) technique.[8,9] Conformal coated self-assembling highly crystalline NKN films were grown on slightly textured and even amorphous substrates due to simultaneous stoichiometric material transfer and resputtering of unproperly oriented crystallites by laser plasma.[8] Changing the ambient oxygen pressure, PLD-grown NKN films were tailored from superparaelectric to strong ferroelectric state.[9] Later on, voltage tunable dielectric permittivity was exploited to fabricate and test NKN microwave varactors[10] as well as to demonstrate electro-optic effect and waveguiding in epitaxial rf-sputtered

NKN films.[11] Since 2000, number of papers, especially on Li and Ta substituted NKN, grows exponentially.

Herein, we report properties of NKN nanofibers sintered by sol-gel electrospinning. The process requiring neither catalysts nor templates yields dense homogeneous ferroelectric nanofiber mat. Being used as an implant, piezoelectric NKN fibers to a certain degree could promote a tissue growth.

To prepare NKN precursor solution, sodium NaO$_2$C$_2$H$_3 \times$ H$_2$O and potassium KO$_2$C$_2$H$_3 \times$ H$_2$O acetates were mixed in 2-methoxyethanol at room temperature and stirred for 1 h to achieve a clear and transparent solution. Niobium ethoxide C$_{10}$H$_{25}$NbO$_5$ was dissolved at room temperature in acetyl acetone (used as a chelating agent), stirred for 1 h, then added to the Na/K precursor solution, and continued stirring for 12 h in a closed cap glass ware. Polyvinylpyrrolidone (PVP, 0.035 g/ml) was added to the precursor mixture to prepare the solution for electrospinning.

Viscous polymer jet was ejected from the syringe pump that feeds PVP/NKN solution at a constant rate of 0.5 ml/hour in electric field 1.8 kV/cm between metallic needle and aluminum foil collector located 8 cm below the tip. Bead-free nanofibers mat was collected from the surface of the collector, dried at 100 °C in nitrogen atmosphere for 12 h, and annealed at 800 °C for 1 h in air.

Scanning electron micrographs (SEM, Fig. 1) collected with field emission microscope *ZIESS Ultra* 55 reveal fibers morphology. After drying at 100 °C in N$_2$, as-spun mat consists of interlaced binder-contained jelly-like threads 350 nm in diameter, stuck with each other [Fig. 1(a)]. They have a smooth surface and amorphous structure. During annealing at 800 °C in air, a polymer binder vaporizes, and threads experience strong shrinkage and transform to the crystallized woven fibers with the average diameter of 150 nm [Fig. 1(b)]. Inset to Fig. 1(b) displays a rough surface of calcined fibers. NKN plate-like nanocrystals grow on top of each other assembling themselves into fibers with several hundreds microns in length. AFM image of individual nanofiber in Fig. 2 reproduces cube-on-cube crystallites growth.
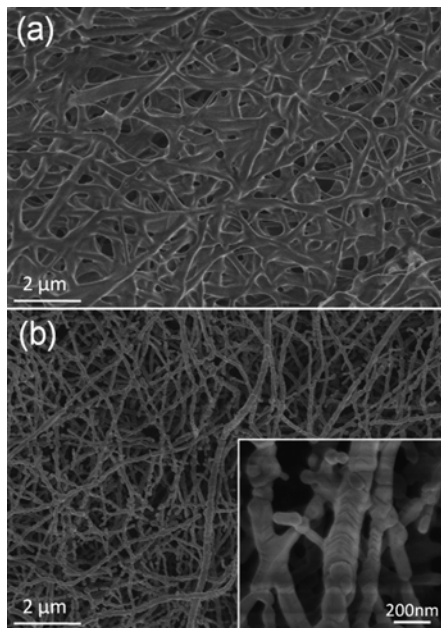
a)Electronic mail: grishin@kth.se.

FIG. 1. SEM images of (Na,K)NbO$_3$ nanofibers: (a) as-spun binder-contained fiber mat after drying at 100 °C in N$_2$ atmosphere, (b) nanofibers calcined at 800 °C in air.

Phase content and crystalline structure of NKN fibers were examined by x-ray diffraction (XRD) using a *Siemens* D-5000 powder diffractometer. Θ-2Θ scan in Fig. 3 confirms a single perovskite phase of the fibers calcined in air at 800 °C for 1 h. The relative intensity ratios of Bragg reflections I_{hkl} indicate noticeable preferential NKN(001) orientation: $I_{001}/I_{011} = 0.86$ in NKN fibers compared to 0.58 in "ideal" Na$_{0.35}$K$_{0.65}$NbO$_3$ powder.[12] This observation conforms to [001]-directional cube-on-cube growth of nanocrystals visualized by SEM in Fig. 1(b) and AFM in Fig. 2. Full width at half maximum (FWHM) $\delta 2\Theta \approx 0.4°$ of (011) peak at $2\Theta = 31.9°$ being substituted to Scherrer formula yields crystallites size of 210 nm which is comparable to the lateral size of nanofibers in SEM images. Insets to Fig. 3 show enlarged (011) and (022) peaks at $2\Theta = 31.9°$ and 66.6° fitted by four Lorentzian lines which present (011) and (022) Bragg manifolds characteristic for monoclinic crystal system in Na$_{0.35}$K$_{0.65}$NbO$_3$ (JCPDS 77-0038 (Ref. 12)). Within each

manifold, individual peaks have the same FWHM: $\delta 2\Theta = 0.06°$ in (011) and 0.11° in (022), and their relative intensities are close to those in monoclinic Na$_{0.35}$K$_{0.65}$NbO$_3$.

Unpolarized backscattered Raman spectra of NKN fibers were recorded at room temperature using a confocal *Jobin Yvon LabRam* HR800 microscope with a CCD detector and 514.5 nm light pumping from an Ar$^+$ laser. According to Kakimoto,[13] Raman scatterings in a wide range 200-900 cm^{-1} are attributed to internal vibrations of NbO$_6$ octahedra in NKN: stretching $1A_{1g}(\nu_1)$, $1E_g(\nu_2)$, $1F_{1u}(\nu_3)$, and bending $1F_{1u}(\nu_4)$, $F_{2g}(\nu_5)$ modes. In Fig. 4, Raman spectrum of fibers annealed at 800 °C clearly resolves six bands fitted to Lorentzian functions which characteristics are collected in Table I. They unambiguously evidence for ferroelectric state of NKN nanofibers.

Recently Kakimoto studied ferroelectric domains in piezoelectric NKN single crystals.[14,15] The sequence of phase transitions from cubic paraelectric phase to ferroelectric

FIG. 3. (Color online) XRD patterns in CuK$_\alpha$ radiation of nanofibers annealed at 800 °C in air. NKN Bragg reflections are notified by Miller indices for pseudo-cubic crystal unit cell. Insets show enlarged (011) and (022) reflections: circular symbols $\bigcirc$ depict experimental XRD pattern whereas solid lines show separate Lorentzian peaks and summarizing fitting curve.
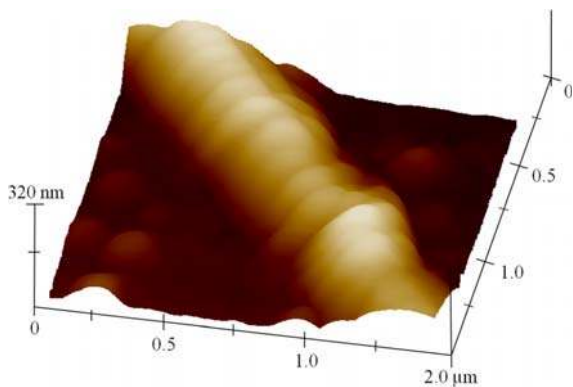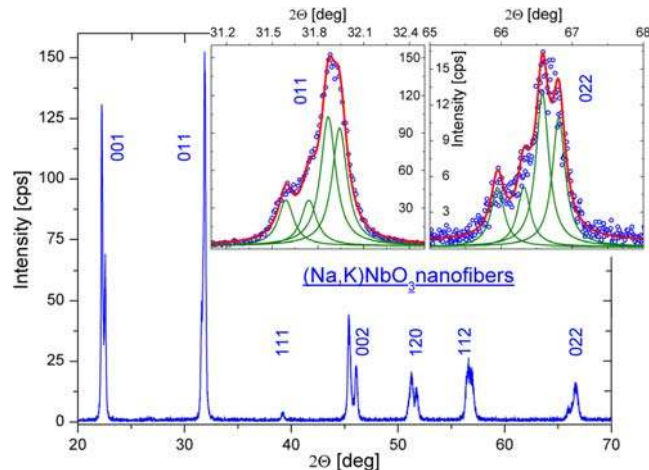

FIG. 2. (Color online) AFM topographical image of an individual (Na,K)NbO$_3$ nanofiber annealed at 800 °C in air.
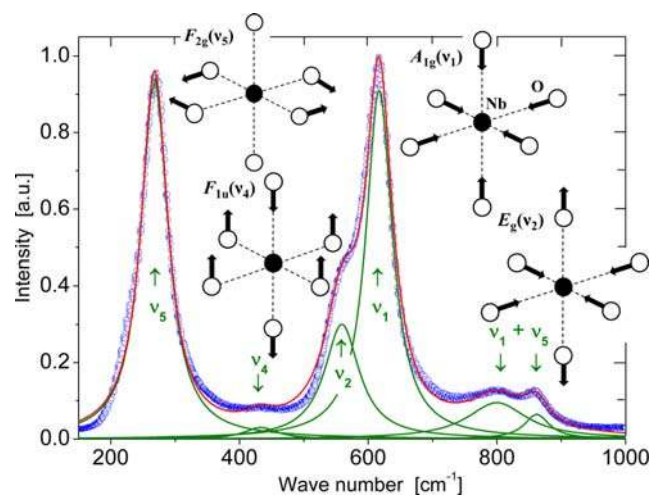

FIG. 4. (Color online) Experimental Raman spectrum of the NKN-nanofibers annealed at 800 °C for 1 h in air is shown with a circular symbols $\bigcirc$. Solid lines depict six separate Lorentzian contours (their characteristics are presented in Table I) and summarizing fitting curve.

tetragonal phase at 407 °C and then from tetragonal to orthorhombic at 170 °C have been traced by Raman spectroscopy and ferroelectric domains observation (see also Ref. 16). The following changes of Raman spectrum accompanied tetragonal-to-orthorhombic phase transition: $v_1(620\,cm^{-1})$ mode became sharper, $v_2(565\,cm^{-1})$ mode appeared and split from $v_1(620\,cm^{-1})$. All the features characteristic to orthorhombic phase are present in Raman spectrum of NKN fibers. Moreover, due to much better crystalline quality of nanofibers evidenced by XRD, they have distinct v_1, v_4, and $v_5(862\,cm^{-1})$ Raman peaks compared to NKN single crystals grown by slow-cooling self flux method.[15]

Comparing spectra in nanofibers, bulk ceramics,[13] and crystals[15] we arrived to the conclusion that stretching $A_{1g}(v_1)$ vibration that corresponds to oscillations of the volume of NbO_6 octahedra has bigger Raman cross section in fibers compared to bulk samples. Really, relative intensity of $v_1(617\,cm^{-1})$ mode increased almost twice compared with $v_5(268\,cm^{-1})$ and $v_2(559\,cm^{-1})$ vibrations, $v_4(433\,cm^{-1})$ mode became noticeable, as well as $v_1(800\,cm^{-1})$, and $v_5(862\,cm^{-1})$ merged in bulk samples split in fibers. This effect unambiguously relates to enhanced isotropic electric polarizability which in its turn might indicate a superparaelectric state of NKN nanofibers.

In paraelectric state according to Langevin, both polarization P and electric polarizability α

$$P = \frac{Np_o^2}{3kT}E, \quad \alpha = \frac{\partial P}{\partial E} = \frac{Np_o^2}{3kT} \quad (1)$$

are isotropic and proportional to a square of the dipole moment p_o and dipoles concentration N (E is electric field, k is a Boltzman constant, and T is the temperature). In ferroelectric state, standard Weiss mean field theory gives the following expression for the longitudinal (parallel to the polar axis) polarizability of uniaxial crystals $\alpha_{\parallel}$[17]

$$\alpha_{\parallel} = \begin{cases} \dfrac{Np_o^2}{3k(T-T_c)}, & T \geq T_c \\ \dfrac{1}{2} \cdot \dfrac{Np_o^2}{3k(T_c-T)}, & T < T_c \end{cases}. \quad (2)$$

Equation (2), known as "rule of two,"[18] describes the λ-shape of the temperature dependence of $\alpha_{\parallel}$ in the vicinity of Curie point $T = T_c$. Bifurcation of paraelectric state into two identical ferroelectric states (domains) causes twice lower magnitude of the low temperature wing of longitudinal polarizability.

TABLE I. Basic parameters of six Raman bands of $(Na,K)NbO_3$ nanofibers.

Mode	Wave number [cm^{-1}]	Peak intensity [a.u.]	Bandwidth [cm^{-1}]	Integral band intensity [a.u.]
v_5	268	0.95	25	74.623
v_4	433	0.03	30	2.83
v_2	559	0.30	33	31.10
v_1	617	0.91	25	71.47
v_1	800	0.095	56	16.71
v_5	862	0.065	23	4.70

The above mentioned results have the following relation to a Raman spectroscopy. In ferroelectric state a symmetry of stretching $E_g(v_2)$ and bending $F_{2g}(v_5)$ vibrations is controlled by the direction of well defined polar axis (shown as a vertical line in $E_g(v_2)$ and $F_{2g}(v_5)$ insets in Fig. 4). Therefore, Raman cross sections of these modes are proportional to longitudinal polarizability $\alpha_{\parallel}$ whereas isotropic component of α determines the cross section of $A_{1g}(v_1)$ vibration.

We believe spontaneous electric polarization inside highly crystalline nanofiber occurs at the critical temperature T_c though a distance between fiber neighbors is too big to settle net macroscopic polarization. In other words, Curie point for whole fiber textile is located at much lower temperatures than T_c. As a result, NKN fiber textile responds to external electric field as a superparaelectric—ensemble of non-interacting electrical dipoles with a large effective dipole moment p_o. In superparaelectric state, the ratio between isotropic and uniaxial components of electric polarizability is defined as $\alpha/\alpha_{\parallel} = 2(T_c/T - 1)$. If we suggest Curie temperature in NKN fibers about 400 °C ($T_c \sim 673\,K$), then at room temperature $\alpha/\alpha_{\parallel}$ becomes equal to 2.5. This can be considered as a qualitative explanation of the enhanced by a factor of two intensity of isotropic $A_{1g}(v_1)$ band observed in Raman spectrum of nanofibers.

In conclusion, the electrospinning of a sodium acetate/potassium acetate/niobium ethoxide/PVP sol-gel and following calcination result in a dense bead-free textile containing highly crystalline $(Na,K)NbO_3$ nanofibers of hundred micrometers in length and 50-200 nm in diameter. Biocompatible piezoelectric fiber mat can be used as electrically polarizable scaffold for engineering, repair, and regeneration of damaged tissue.

[1]B. T. Matthias, Phys. Rev. **75**, 1771 (1949).
[2]G. Shirane, R. Newnham, and R. Pepinsky, Phys. Rev. **96**, 581 (1954).
[3]L. Egerton and D. M. Dilllon, J. Am. Ceram. Soc. **42**, 438 (1959).
[4]R. H. Dungan and R. D. Golding, J. Am. Ceram. Soc. **48**, 601 (1965).
[5]K. Nilsson, J. Lidman, K. Ljungstrom, and C. Kjellman, U.S. patent 6,526,984 (4 March 2003).
[6]A. M. Margolin, Z. S. Surovyak, I. N. Zakharchenko, V. A. Aleshin, L. K. Chernysheva, M. G. Radchenko, and V. P. Dudkevich, Sov. Phys. Tech. Phys. **33**, 1435 (1988).
[7]X. Wang, U. Helmersson, S. Olafsson, S. Rudner, L. D. Wernlund, and S. Gevorgian, Appl. Phys. Lett. **73**, 927 (1998).
[8]C.-R. Cho and A. M. Grishin, Appl. Phys. Lett. **75**, 268 (1999).
[9]C.-R. Cho and A. M. Grishin, J. Appl. Phys. **87**, 4439 (2000).
[10]C.-R. Cho, J.-H. Koh, A. Grishin, S. Abadei, and S. Gevorgian, Appl. Phys. Lett. **76**, 1761 (2000); J.-Y. Kim and A. M. Grishin, Appl. Phys. Lett. **88**, 192905 (2006).
[11]M. Blomqvist, J.-H. Koh, S. Khartsev, A. Grishin, and J. Andréasson, Appl. Phys. Lett. **81**, 337 (2002); M. Blomqvist, S. Khartsev, A. Grishin, A. Petraru, and C. Buchal, Appl. Phys. Lett. **82**, 439 (2003); S. I. Khartsev, M. A. Grishin, and A. M. Grishin, Appl. Phys. Lett. **86**, 062901 (2005).
[12]Hereinafter we notify NKN Bragg reflections using Miller indices in pseudo-cubic crystal system. This unit cell is twice downsized monoclinic Bravais lattice from 2001 JCPDS-International Center for Diffraction Data, Card No. 77-0038 ($Na_{0.35}K_{0.65}NbO_3$).
[13]K. Kakimoto, K. Akao, Y. Guo, and H. Ohsato, Jpn. J. Appl. Phys. **44**, 7064 (2005).

[14]Y. Inagaki and K. Kakimoto, Appl. Phys. Express **1**, 061602 (2008).

[15]Y. Inagaki, K. Kakimoto, and I. Kagomiya, J. Am. Ceram. Soc. **93**, 4061 (2010).

[16]N. Klein, E. Hollenstein, D. Damjanovic, H. J. Trodahl, N. Setter, and M. Kuball, J. Appl. Phys. **102**, 014112 (2007); H. J. Trodahl, N. Klein, D. Damjanovic, N. Setter, B. Ludbrook, D. Rytz, and M. Kuball, Appl. Phys. Lett. **93**, 262901 (2008).

[17]A. M. Grishin and A. N. Ulyanov, Fiz. Tverd. Tela (Phys. Solid State), **27**, 237 (1985).

[18]V. L. Ginzburg, Zhurnal Éksperimental'noĭ i Teoreticheskoĭ Fiziki (JETP, J. Exp. Theor. Phys.) **17**, 831 (1947).